Available online at www.sciencedirect.com

SCIENCE DIRECT®

Polymer 45 (2004) 2921–2929

polymer

www.elsevier.com/locate/polymer

Photopolymerization of pigmented thiol–ene systems

T.M. Roper[a], T. Kwee[a], T.Y. Lee[a], C.A. Guymon[b], C.E. Hoyle[a,*]

[a]*Department of Polymer Science, University of Southern Mississippi, Box 10076, Hattiesburg, MS 39406-0076, USA*
[b]*Department of Chemical and Biochemical Engineering, University of Iowa, Iowa City, IA 52242, USA*

Received 3 November 2003; received in revised form 6 November 2003; accepted 18 February 2004

Abstract

Photopolymerization kinetics and optical properties of pigmented thiol–ene coatings were investigated using photo-DSC, real-time FTIR, colorimetry, and AFM. Pigment has no deleterious effect on the unique ability of thiol–ene systems to photopolymerize in air. When trimethylolpropane tris-(3-mercaptopropionate) is incrementally added to tripropylene glycol diacrylate with and without calcium lithol rubine, a red organic pigment, the photopolymerization rate in nitrogen steadily decreases due to a shift in the polymerization mechanism from an acrylate homopolymerization to a thiol–ene copolymerization. However, the photopolymerization rate of pigmented and non-pigmented systems in air significantly increases with increasing thiol concentration, ultimately reaching a maximum at approximately 35 mole percent trifunctional thiol. The increase in rate is due to chain transfer from the non-reactive peroxy radical to the thiol. Thiol groups reduce oxygen inhibition to a greater degree than standard additives such as *N*-methyldiethanolamine, *N*-vinyl pyrrolidinone, and thioether containing trifunctional vinyl esters. For a typical acrylate based pigmented photocurable system, greater than 10 wt% photoinitiator is required to achieve a photopolymerization rate equivalent to a comparable thiol–ene system with 1 wt% photoinitiator in air. AFM and colorimetric data indicate that addition of trifunctional thiol has no deleterious effect on pigment dispersion and may in fact increase dispersion quality.

Keywords: Kinetics; Photopolymerization; Thiol–ene

1. Introduction

Photopolymerization is an efficient, environmentally friendly, and economically favorable method to produce coatings which can display a wide range of properties depending on the identity of reactive species and additives employed. Since its inception, pursuit of additional applications has been a driving force behind academic and industrial research and is responsible for the continued development of photopolymerizable thiol–enes [1–5]. Thiol–ene polymers are formed through reaction of multifunctional thiol with a multifunctional ene, where the ene is a carbon–carbon double bond. A linear polymer is formed upon reaction of difunctional thiol with difunctional ene, whereas a crosslinked polymer is formed when either the thiol or ene has a functionality greater than two. First examined extensively in the 1970’s, thiol–enes continue to serve as an alternative to acrylate photopolymerizations [6–8]. Thiol–ene systems are unique in that they photopolymerize rapidly in air, in contrast to traditional photopolymerizable free-radical formulations which are normally substantially inhibited by oxygen [7–10].

Thiol–enes follow a step-growth addition mechanism consisting of a two-step propagation sequence as illustrated in Fig. 1 [1,6,10]. The thiyl radical, generated from a thiol through direct excitation by ultraviolet radiation or hydrogen abstraction by a cleavage type photoinitiator, inserts into both electron rich and electron poor carbon–carbon double bonds. The subsequent carbon centered radical then abstracts a thiol hydrogen to regenerate the thiyl radical and complete the two-step propagation sequence. The step growth nature of the polymerization produces a uniformly cross linked network only at high conversion resulting in reduced overall shrinkage and excellent adhesion. Thiol–enes are versatile systems because of the variety of enes one may select as a co-reactant with the thiol. Double bonds from acrylates, vinyl ethers, allyl ethers, norbornenes, and unsaturated hydrocarbons all polymerize with multifunctional thiol [10].

---

[*] Corresponding author. Tel.: +1-601-266-4868; fax: +1-601-266-5504.
E-mail address: charles.hoyle@usm.edu (C.E. Hoyle).

0032-3861/$ - see front matter © 2004 Elsevier Ltd. All rights reserved.
doi:10.1016/j.polymer.2004.02.038

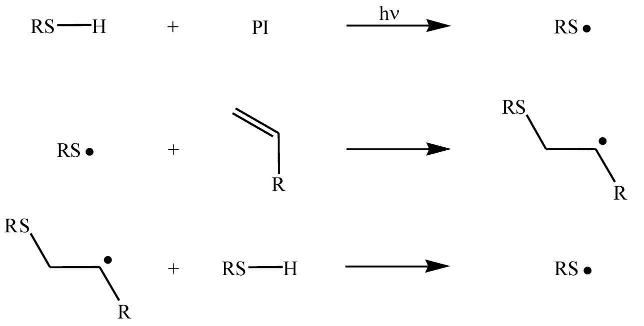

Fig. 1. Thiol–ene propagation sequence.

Photopolymerizable thiol–ene systems have found use in a variety of clear-coating applications for the reasons described above. Pigmented photopolymerizable inks/coatings, which are often plagued by slow polymerization rates in air, represents a growing field that could significantly benefit from the unique properties offered by thiol–ene technology. Photocurable inks are composed of pigment dispersed in a reactive mixture including monomer/oligomer and photoinitiator. Organic pigments are generally used because they impart extremely intense color and are relatively easy to wet/disperse with most reactive monomers/oligomers. Pigment produces specific colors within the coating by selectively absorbing and scattering incident radiation. As a result of this interaction with light, the photopolymerization rate decreases as the pigment competes with the photoinitiator for available photons [11–13]. A photoinitiator must be selected that absorbs wavelengths of light where the pigment has an absorbance minimum to allow sufficient photopolymerization rates [11–14]. Pigment will also scatter all incident wavelengths of light, thereby preventing light from penetrating the system and subsequently decreasing the concentration of free-radicals and reducing polymerization through the coating. Because of the inherently slow polymerization of pigmented systems, extreme measures must be taken to increase the polymerization rate in air such as nitrogen purging, addition of small molecule oxygen scavengers and high photoinitiator(s) concentrations [11–13,15,16]. Nitrogen purging is expensive and use of excess photoinitiators or small molecule oxygen scavengers is undesirable since they may diffuse out of the coating or degrade over time restricting product applications [17].

Since thiol–ene photocurable coatings are relatively insensitive to oxygen inhibition, their incorporation in pigmented systems may lead to enhanced polymerization rates in air. In this study, real-time infrared spectroscopy and photo-differential scanning calorimetry are used to examine the effect that multifunctional thiols have on the photopolymerization rate of pigmented acrylate formulations in nitrogen and air. In addition, pigmented thiol–acrylate systems are compared to pure acrylate formulations modified with traditional additives for enhancing polymerization rates in air. Interactions between the thiol and pigment may lead to changes in the pigment dispersion that affect color strength. Therefore, the pigment dispersion stability upon addition of thiol is examined using AFM and colorimetry.

2. Experimental

2.1. Materials

The ene monomers with reactive carbon–carbon double bonds included the diacrylate, tripropylene glycol diacrylate (TRPGDA—UCB Chemicals Corp.) as well as a trivinyl ester (TVE). The thioether containing trivinyl ester was synthesized by adding trimethylolpropane tris-(3-mercaptopropionate) to vinyl acrylate in the presence of a primary amine catalyst [18]. The trifunctional thiol used in these studies was trimethylolpropane tris-(3-mercaptopropionate) (trithiol—Aldrich). The photoinitiator and red organic pigment utilized were 2,2-dimethoxy-2-phenyl acetophenone (DMPA—Ciba Specialty Chemicals) and calcium lithol rubine (Flint Ink Corp.). *N*-Vinyl pyrrolidinone (NVP) and N-methyldiethanolamine (MDEA) were examined in comparison to the thiol for reducing oxygen inhibition in pigmented systems. The relevant chemical structures are shown in Fig. 2. All chemicals were used as received, without additional purification.

2.2. Methods

UV–Vis spectra were measured using a Cary 500 UV–Vis-NIR spectrophotometer. All samples were prepared using acetonitrile as a solvent in a 1 cm pathlength quartz cuvette. Pigment spectra were obtained after dispersing the pigment in acetonitrile on a ball mill for 2 h.

A photo-differential scanning calorimeter (photo-DSC) was used to collect the photopolymerization exotherms, which are proportional to the maximum rate of polymerization. The photo-DSC was constructed from a Perkin Elmer DSC 7 by modifying the DSC head with quartz windows. A 450 W medium pressure mercury lamp from Ace Glass served as the light source and was shielded from the DSC head by an electric shutter. Pigmented samples were dispersed on the ball mill for one hour prior to all kinetic experimentation. Samples of 2.00 ± 0.03 mg were weighed into crimped aluminum sample pans. Samples polymerized in an inert atmosphere were purged with nitrogen for four minutes before irradiation. Sample thicknesses were between 175 and 200 μm.

A Bruker IFS 88 modified to accommodate a horizontal sample accessory was used to collect real-time infrared spectroscopic data of photopolymerizations. Ultraviolet light from an Oriel lamp system equipped with a 200 W high pressure mercury xenon bulb was channeled through an electric shutter and fiber optic into the sample chamber. Photopolymerizations in nitrogen were conducted by

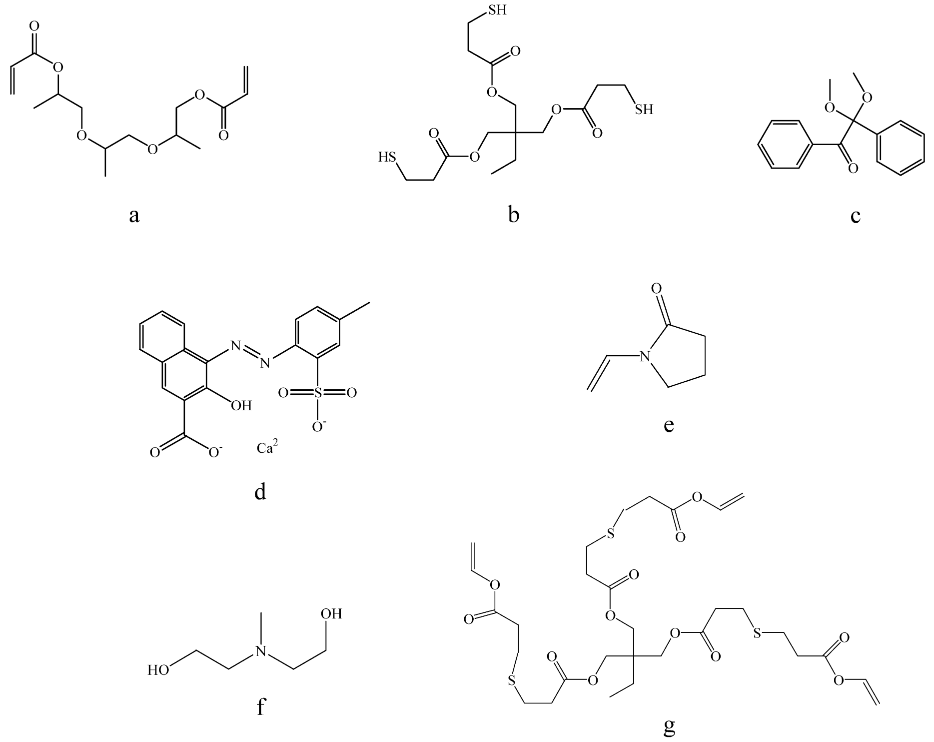

a b c

d e

f g

Fig. 2. Chemical structures of (a) tripropylene glycol diacrylate (TRPGDA), (b) trimethylolpropane tris-(3-mercaptopropionate) (Trithiol), (c) 2,2-dimethoxy-2-phenyl acetophenone (DMPA), (d) calcium lithol rubine, (e) *N*-vinyl pyrrolidinone (NVP), (f) *N*-methyldiethanolamine (MDEA), and (g) trivinyl ester (TVE).

sandwiching the sample between two sodium chloride salt plates at a thickness of approximately 20 μm and purged 10 min in nitrogen prior to irradiation. For photopolymerization in air, a drill press was used to form a pocket which held a sufficient air supply between the sandwiched salt plates. The 812 cm^{-1} absorbance band from the acrylate double bond was monitored during the polymerization. The area from this peak was used to calculate percent conversion as shown below, where A_0 is the initial area of the 812 cm^{-1} peak and A_t is its area at any time, t, after exposure to UV radiation:

$$\text{Conversion} = [A_0 - A_t]/A_0$$

Colorimetric data in the CIELAB color space was collected on cured films using a BYK Gardner Color-Guide 45/0 (CIELAB D65/10). Films were prepared on aluminum substrates at a thickness of 4 mils (100 μm) and purged 10 min in a nitrogen purge UV cure line cell. The cell was then immediately cured with five passes on a Light Hammer 6 UV cure system with each pass giving a total dose of 0.26 J/cm^2. All reported color measurements are the average of three measurements.

Following colorimetric measurements, morphology and pigment dispersion of the films were examined using Atomic Force Microscope (AFM). Tapping-mode AFM was performed using a Digital Instrument Dimension 3000 Nanoscope IIIa. The resulting phase images were due to the difference between the input and output force response associated with the difference in the local mechanical properties between the hard and soft regions. The applied tapping frequency was approximately 2 Hz. In order to minimize artifacts, all bulk sample surfaces were smoothed using a glass knife prior to phase image acquisition. The tapping mode was used to preserve the surface topography of the sample and thus increase reproducibility. Bright and dark images shown in the phase images can be attributed to the pigment clusters and polymer matrix, respectively.

3. Results and discussion

Photopolymerization rates of pigmented inks/coatings are plagued by a reduction in the effective light intensity due to the competition between the pigment and photoinitiator for photons of light. As a result, fewer free radicals are created thereby magnifying the effect of oxygen inhibition in these systems. The potential benefit of thiol in a pigmented photopolymerizable system is significant since thiol–ene photocurable coatings are relatively insensitive to oxygen. To test this hypothesis, trithiol is incrementally added to a mixture of difunctional acrylate, photoinitiator, and pigment to examine the possibility of increasing the polymerization rate of pigmented systems in air. Trimethylolpropane tris-(3-mercaptopropionate) (trithiol) was selected for its commercial availability and its ability to produce a crosslinked network upon reaction with tripropylene glycol diacrylate (TRPGDA). TRPGDA is a difunctional ene that stabilizes the pigment dispersion and displays fast polymerization rates. To eliminate potential initiation by the thiol, 365 nm light is used in most kinetic measurements [5]. The photoinitiator, 2,2-dimethoxy-2-phenyl acetophenone (DMPA), is a cleavage type photoinitiator that absorbs significantly at 365 nm as shown in Fig. 3.

Addition of pigment to a photocurable formulation decreases the rate of polymerization by reducing the photons available to initiate polymerization [11–13]. Polymerization rates of pigmented systems can be extremely slow, and attempting rate measurements can test the limitations of traditional instrumentation such as the photo-DSC. Therefore, the pigment to be used for analysis in the thiol–ene systems should exhibit fast polymerizations and consequently generate large polymerization exotherms that are accurate and reproducible. Calcium lithol rubine, a red organic pigment, is a likely candidate because its absorbance at 365 nm, the initiating wavelength, is significantly lower than other organic pigments. In addition, only 5 wt% pigment of the total resin was added to ensure maximum monomer conversion upon irradiation, whereas typical photocurable inks will contain up to 20 wt% pigment. Calcium lithol rubine as received is a dry powder that, according to particle size analysis, has an average particle size of 167.4 μm. To make efficient use of the pigment and produce intense color, the pigment particles were milled to an average particle size less than 1 μm using a ball mill.

To verify that the components chosen will allow rapid polymerization rates accurately detectable by the photo-DSC, UV–Vis absorbance spectra of the photoinitiator and pigment were collected and compared. Fig. 3 shows the UV–Vis absorbance spectra for calcium lithol rubine and DMPA. In addition to the expected broad absorbance in the visible for a red pigment from 450 to 650 nm, the pigment strongly absorbs ultraviolet light below 315 nm. Consequently, it is extremely difficult to photopolymerize coatings containing this pigment using light below 315 nm. DMPA displays an absorbance peak at 340 nm, extending from less than 300 nm to approximately 400 nm and overlapping a relative absorbance minimum for the calcium lithol rubine. Therefore, DMPA, at appropriate concentrations, should initiate photopolymerization of a photocurable acrylate incorporating calcium lithol rubine at appropriate concentrations when exposed to the 365 nm band from of a medium or high pressure mercury arc lamp.

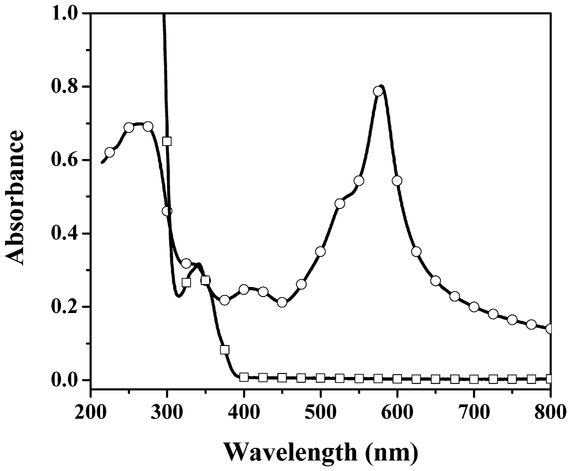

Fig. 3. UV–Vis absorbance spectra of 0.0007 M DMPA (□) and 0.0012 M calcium lithol rubine (○) in acetonitrile.

Oxygen inhibition of free-radical polymerizations is a deterrent for many potential applications of photopolymerization. Oxygen significantly inhibits the polymerization by reacting with both initiating and propagating free radicals to generate stable peroxy radicals resulting in termination of polymerization [15–17]. Thiol has been reported to reduce the effects of oxygen inhibition by undergoing chain transfer with the peroxy radical to produce a hydrogen peroxide and thiyl radical which can initiate polymerization. This prevents depletion of propagating free radicals and allows polymerization to occur in air [4,7,8,10]. Photo-DSC exotherms illustrating the effect of trithiol on the polymerization of TRPGDA in air are depicted in Fig. 4. TRPGDA homopolymerization proceeds in nitrogen ultimately reaching a maximum heat release of 80 mW. However, the same polymerization attempted in air undergoes no reaction due to oxygen inhibition. Addition of 30 mol% trithiol to TRPGDA results in about 75% recovery of the maximum heat released for TRPGDA homopolymerization in nitrogen, virtually eliminating the effect of oxygen on the polymerization.

From these results it is evident that thiol substantially reduces oxygen inhibition in TRPGDA. On the other hand, 30 mol% trithiol may be more than is necessary to achieve appropriate rates. To determine the optimum thiol concentration in reducing oxygen inhibition, trithiol was incrementally added to TRPGDA polymerizations in air and nitrogen. Fig. 5 shows a plot of the maximum rate of heat

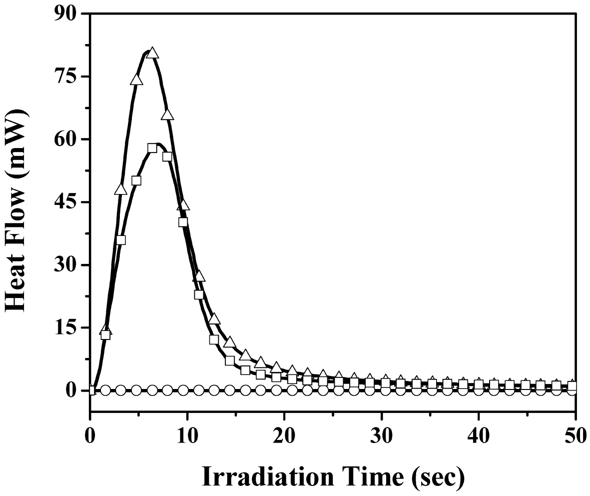

Fig. 4. Photo-DSC exotherms of TRPGDA in nitrogen (△), air (○), and with 30 mol% trithiol in air (□). Samples contain 1 wt% DMPA and were polymerized at a light intensity of 0.6 mW/cm^2 using 365 nm light.

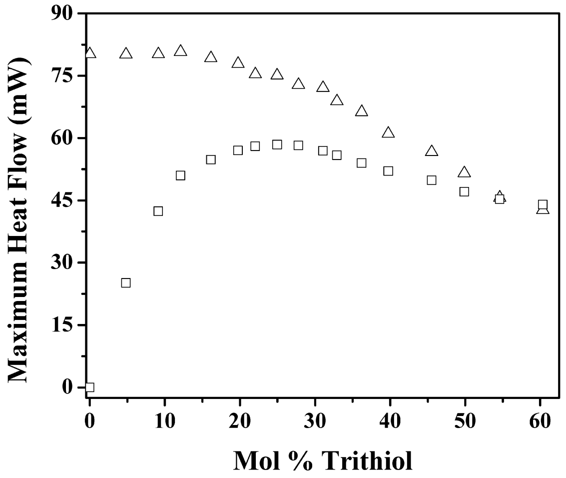

Fig. 5. Maximum photo-DSC exotherm values for TRPGDA samples containing 1 wt% DMPA as a function of trithiol content. Samples were polymerized in nitrogen (△) and air (□) at a light intensity of 0.6 mW/cm^2 using 365 nm light.

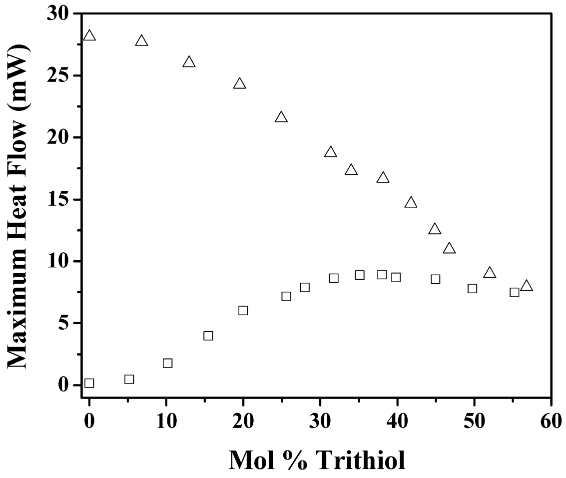

Fig. 6. Maximum photo-DSC exotherm values for TRPGDA samples containing 1 wt% DMPA and 5 wt% calcium lithol rubine as a function of trithiol content. Samples were polymerized in nitrogen (△) and air (□) at a light intensity of 0.6 mW/cm^2 using 365 nm light.

release for TRPGDA polymerizations conducted in air and nitrogen purged samples as a function of trithiol content. Interestingly, as little as 5 mol% trithiol results in a significant increase in the maximum rate of heat released. The maximum rate of heat released increases with increasing trithiol content until approximately 30 mol% trithiol, at which point the thiol–ene polymerization rate in air approaches the polymerization rate in nitrogen. Subsequent addition of trithiol results in a decrease in the maximum rate of heat released similar to the decrease observed when trithiol is added to TRPGDA polymerized in nitrogen. The lower exotherm rates with increasing thiol content in nitrogen are due to a change in mechanism from pure acrylate homopolymerization in the absence of thiol to a combination of a thiol–acrylate copolymerization and acrylate homopolymerization [7,8,10]. The combination has an overall lower polymerization rate than the pure TRPGDA homopolymerization, as the rate of adding thiol across the acrylate bond is slower than acrylate homopolymerization.

In order to assess the possibility of formulating a photocurable pigmented acrylate system that cures in air, the impact of trithiol on photopolymerization of pigmented systems is also important to examine. Fig. 6 depicts a plot of the maximum rate of heat release for TRPGDA polymerizations containing 5 wt% calcium lithol rubine conducted in air and nitrogen as a function of trithiol content. Identical light intensity and photoinitiator concentrations were used in both the current study and the non-pigmented thiol–ene analysis from Fig. 5. As expected the pigment reduces the rate of heat released for systems polymerized in both air and nitrogen compared to the analogous non-pigmented formulation. The rate of heat release for TRPGDA polymerized in nitrogen decreases 65% upon addition of pigment. The decrease in rate is due to a reduction in available photons to initiate polymerization. Fewer radicals are thereby generated reducing the monomer consumption and inducing a slower polymerization rate [11–13].

As the content of trithiol is increased in the pigmented TRPGDA systems polymerized in nitrogen (Fig. 6), the rate decreases due to a change in the mechanism from TRPGDA homopolymerization to a thiol–ene copolymerization as previously discussed. On the other hand, the rate significantly increases and reaches a maximum rate of heat release at approximately 35–40 wt% when polymerized in air. This behavior clearly illustrates that the polymerization rate in air for pigmented coating formulations can be dramatically increased by the addition of thiol. While the pigmented and non-pigmented systems general polymerization behavior appears to be similar, some interesting changes are evident. Subtle differences between the pigmented systems and non-pigmented systems upon addition of trithiol include the magnitude of the decrease in rate for pigmented thiol–ene systems polymerized in nitrogen. Additionally, the increase in rate appears to be delayed for the pigmented systems polymerized in air and the thiol concentration needed to reach maximum rates shifts from 30 to 35% trithiol. These variations may be due to a reduction in the effective light intensity (inner filter effect) and possibly a change in the pigment dispersion. Addition of pigment effectively reduces the light intensity, causing fewer radicals to be generated and possibly altering the polymerization mechanism [11–13]. Increasing the light intensity delivered to the pigmented samples to produce exotherms on the same order as the non-pigmented system, or decreasing the light intensity of the non-pigmented samples, eliminates the disparity in the results. Addition of trithiol may also change the distribution of pigment which could affect the polymerization rate.

Further information regarding polymerization behavior, especially acrylate conversion, could be extremely inundating. Real-time IR (RTIR) has proven an excellent tool for comparative studies of photopolymerizable systems and can be used to complement data collected on the photo-DSC [19–22]. In addition to comparing rates of monomer conversion, RTIR provides a detailed account of the total quantity of monomer converted into polymer. Disappearance of the IR absorbance peak at 812 cm^{-1}, which corresponds to the carbon–carbon double bond in the acrylate group, can be monitored to find conversion as a function of time. The change in IR absorbance for the homopolymerization of TRPGDA with 1 wt% DMPA in a nitrogen purged atmosphere is pictured in Fig. 7 along with the corresponding percent conversion versus time plot. Polymerization proceeds rapidly over the first 15 s and then approaches 90% total conversion after 100 s. As seen in Fig. 7, in general, multifunctional acrylate homopolymerizations are fast and attain high conversion when conducted in nitrogen.

As indicated by this and the previously described photo-DSC data, homopolymerization of TRPGDA in nitrogen is rapid, but the rate decreases substantially with addition of pigment or in air. Fig. 8 clearly shows the effect of oxygen on conversion in the free-radical homopolymerization of TRPGDA as demonstrated using RTIR. In air, TRPGDA does not undergo homopolymerization to any appreciable extent upon irradiating at 365 nm (33 mW/cm^2). The effect of 5 wt% of calcium lithol rubine on the photopolymerization of TRPGDA as monitored in nitrogen is shown in Fig. 8. Both the rate of monomer conversion, which is the slope of the conversion as a function of time plot, and total conversion significantly decrease in the presence of the pigment. The time to reach 60% conversion more than doubles upon the addition of calcium lithol rubine. The inner filter effect and concomitant competitive absorption/scattering of the light by the pigment causes the decrease in rate and conversion with pigment content. Such a reduction in monomer conversion can have a detrimental effect on physical properties such as hardness, abrasion resistance, and scratch resistance.

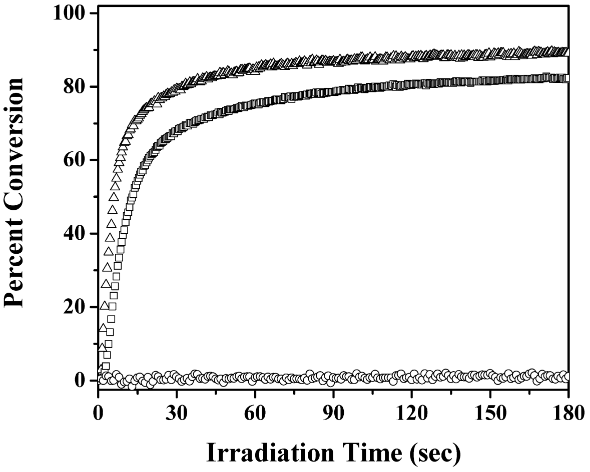

Fig. 8. RTIR conversion plots for TRPGDA in nitrogen (△), in nitrogen with 5 wt% calcium lithol rubine (□), and in air (○). Samples contain 1 wt% DMPA and were polymerized at a light intensity 33 mW/cm^2 using 365 nm light.

Photo-DSC results described previously show an increase in rate for pigmented systems photopolymerized in air as trithiol is added. Complementary RTIR results examining the effect of 30 mol% trithiol on the rate of conversion of TRPGDA containing 5 wt% calcium lithol rubine in air are shown in Fig. 9. As expected the homopolymerization of pigmented TRPGDA in air does not appear to occur due to oxygen inhibition. However, upon addition of 30 mol% trithiol the rate of conversion significantly increases and ultimately the final conversion is equal to or slightly greater than TRPGDA homopolymerization in nitrogen. On the other hand, the initial rate of conversion is slower for the pigmented thiol–ene system polymerized in air than the pigmented TRPGDA system polymerized in nitrogen. This result is no different than the effect observed on the photo-DSC as trithiol is added to TRPGDA in nitrogen and air. The rate decreases due to a shift in mechanism from a fast acrylate homopolymerization to a slightly slower thiol–ene copolymerization. Despite

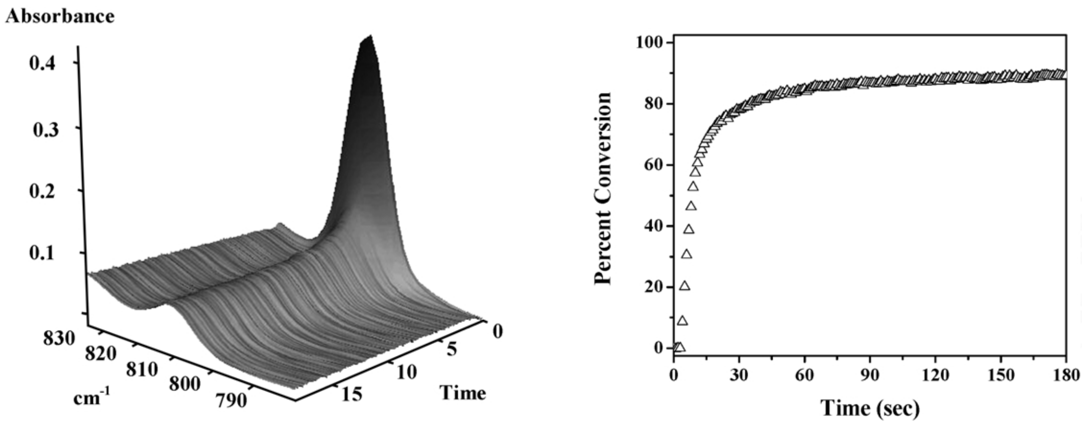

Fig. 7. Three dimensional RTIR image depicting the disappearance of the TRPGDA acrylate double bond at 812 cm^{-1} as a function of time and the corresponding plot of percent acrylate conversion (△) as a function of time. Polymerization conducted in nitrogen with 1 wt% DMPA and a light intensity of 33 mW/cm^2 using 365 nm light.

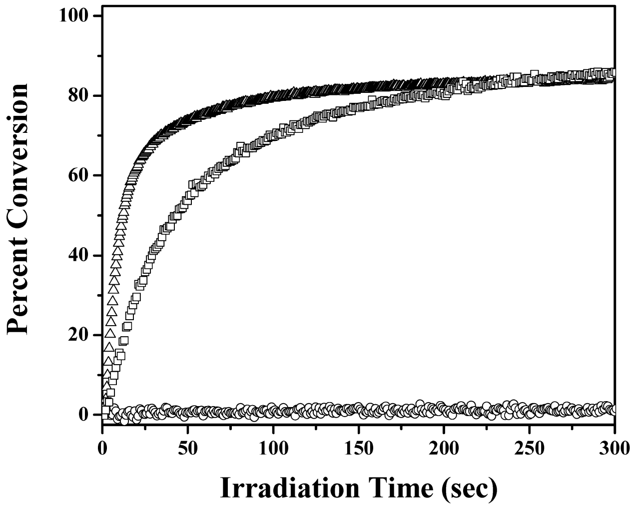

Fig. 9. RTIR conversion plots for TRPGDA in nitrogen (△), in air with 30 mol% trithiol (□), and in air (○). Samples contain 1 wt% DMPA and 5 wt% calcium lithol rubine and were polymerized at a light intensity 33 mW/cm^2 using 365 nm light.

having a slightly slower rate of conversion, the pigmented thiol–ene system ultimately achieves higher monomer conversion. Thiol–ene copolymerizations are step-growth polymerizations and therefore a crosslinked network is not formed until high conversion, whereas pure acrylate polymerizations form crosslinked microgels as early as 5% conversion, trapping non-reacted functional groups in the network. Because of delayed network formation, thiol–enes generally achieve higher conversions and have reduced overall shrinkage upon formation of polymer. In summary, varying the thiol content within an acrylate formulation will not only enable polymerization to occur in air, but also results in higher conversion, which may significantly influence the physical properties of coatings.

Photo-DSC and RTIR results clearly indicate non-pigmented and pigmented thiol–ene systems rapidly photopolymerize in an air atmosphere. To test the effectiveness of thiol–ene systems in the presence of pigment, it is also important to compare various traditional additives for reducing the effect of oxygen inhibition such as N-vinyl-2-pyrrolidinone (NVP) and *N*-methyldiethanolamine (MDEA). Structures for these compounds are shown in Fig. 2. The mechanism by which the traditional additives function has been described in previous literature [15,16]. In addition, a novel trifunctional vinyl ester (TVE) (Fig. 2) containing thioether linkages which have been shown to reduce oxygen inhibition is evaluated [18]. Photo-DSC exotherms of TRPGDA formulations containing equivalent amounts of photoinitiator and pigment with the specified additive are compared in Fig. 10. Interestingly, addition of 35 mol% trithiol to pigmented system results in a considerably larger increase in polymerization rate than the traditional additives as well as the TVE. The exotherm maximum for the pigmented thiol–ene system is approximately 20%, 60%, and 150% greater than the exotherm maximum for the NVP, MDEA, and TVE samples, respectively.

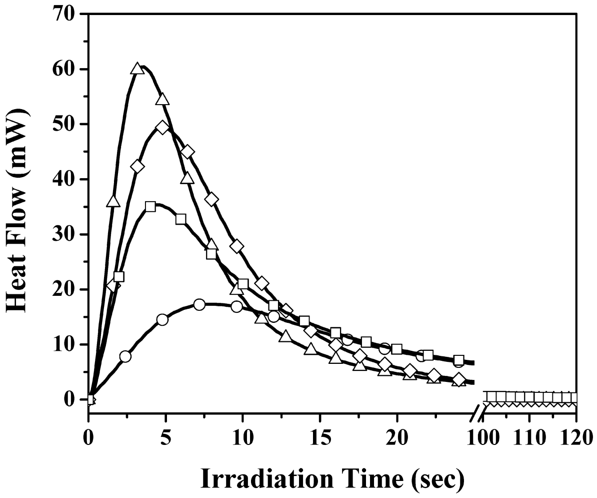

Fig. 10. Photo-DSC of TRPGDA samples in air containing 5 wt% calcium lithol rubine, 1 wt% DMPA and (△) 35 mol% trithiol, (◇) 35 mol% NVP, (□) 2 mol% MDEA, or (○) 30 mol% TVE. Polymerizations were conducted at a light intensity of 99.8 mW/cm^2 using 365 nm light.

A common solution for increasing the photopolymerization rate of pigmented systems in air is addition of high photoinitiator concentrations. In order to determine what concentration of photoinitiator would be required to give the same overall exotherm rate as that attained by the pigmented thiol–ene system in air, the concentration of DMPA was varied until comparable photo-DSC exotherms were observed. As seen in Fig. 11, only after addition of 10 wt% DMPA does the polymerization proceed at an exotherm rate approaching that of the 35 mol% thiol–ene system. This result has far reaching implications for practical photocuring of pigmented coatings. It suggests that equivalent ene rates in air to those achievable only by

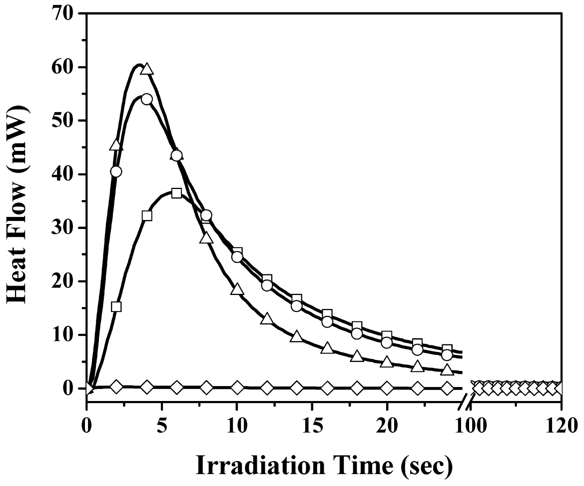

Fig. 11. Photo-DSC exotherms of TRPGDA samples in air containing 5 wt% calcium lithol rubine and 35 mol% trithiol (△), (○) 10 wt% DMPA, (□) 5 wt% DMPA, and (◇) 1 wt% DMPA. Polymerizations were conducted at a light intensity of 99.8 mW/cm^2 using 365 nm light.

use of high photoinitiator concentrations can be obtained by simply adding thiol to pigmented acrylate formulations. Since the thiols are incorporated into the matrix by the thiol–ene reaction, little to no extractable residuals in the final cured films will be present. The results in Fig. 11 using 1 wt% DMPA and 35% thiol/65% TRPGDA mixture are particularly remarkable when considering the thickness of the film (150–200 μm) and the extent of pigment incorporation (5 wt%).

Thus far it has been demonstrated that the advantages conveyed to an acrylate formulation by addition of thiol are maintained in the presence of pigments. When addressing pigmented systems, changes in the formulation that may have a deleterious effect on the color strength must also be considered. Color strength is determined by the inherent properties of the pigment, pigment concentration and the pigment distribution within the coating. Atomic force microscopy (AFM) can be utilized to analyze the pigment dispersion of cured films [23,24]. Furthermore, colorimetry can be used to detect changes in color upon addition of trithiol which are indicative of changes to the pigment dispersion [25]. AFM was conducted on cross sections of photocured pigmented films cured on a benchtop UV cure system. Pure homopolymerized TRPGDA films are extremely difficult to section due to the brittle nature (high glass transition temperature) of the film. Addition of trithiol to TRPGDA decreases the glass transition of the resultant polymer and gives smooth uniform sections which are ideal for analysis as illustrated by the AFM images pictured in Fig. 12 [21]. The pigment particle size is 60 nm on average and remains the same up to 35 mol% thiol indicating that the trithiol has little effect on the pigment distribution. Colorimetric measurements were conducted on the same films to complement the AFM image analysis. Because calcium lithol rubine is a red pigment, the values within the CIELAB color space used to characterize the color were a^* and ΔE. Larger (more positive) a^* values indicate a film with a bright or more intense red color. ΔE is a measure of the color difference between two samples, for which values greater than 1.0 typically indicate a color change detectable by the human eye. As shown in Fig. 13, addition of trithiol to pigmented TRPGDA formulations does not affect the a^* component. In addition, the ΔE values are less than one indicating there is no perceptible change in color. Therefore, addition of thiol to an acrylate formulation containing calcium lithol rubine has little effect on the pigment distribution within the film.

4. Conclusion

The photopolymerization kinetics and color properties of pigmented thiol–ene coatings were investigated using photo-DSC, real time FTIR, colorimetry, and AFM. Pigments reduce the rate of photopolymerization by effectively decreasing the light intensity through competitive absorption of the

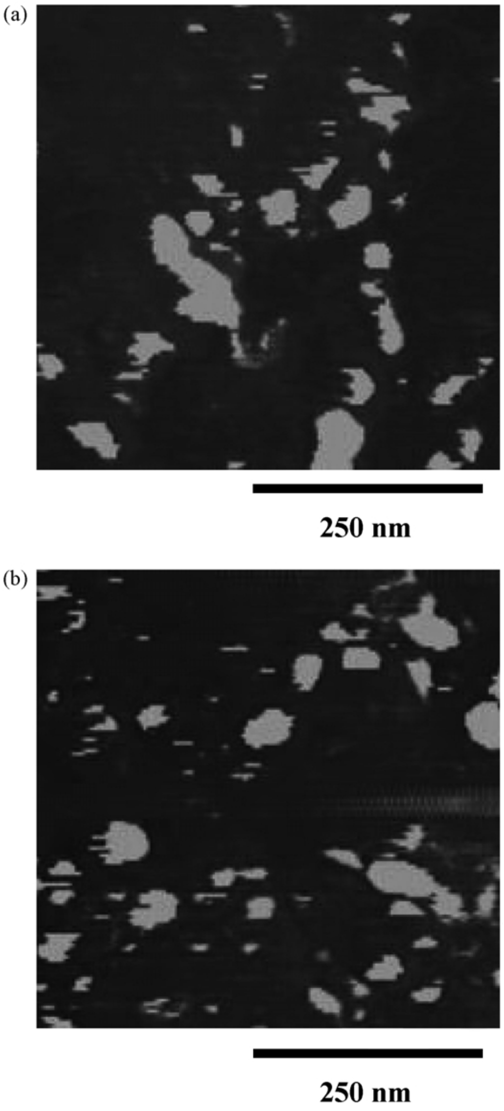

Fig. 12. AFM phase image of TRPGDA films with 5 wt% calcium lithol rubine containing 5 mol% trithiol (a) and 35 mol% trithiol (b).

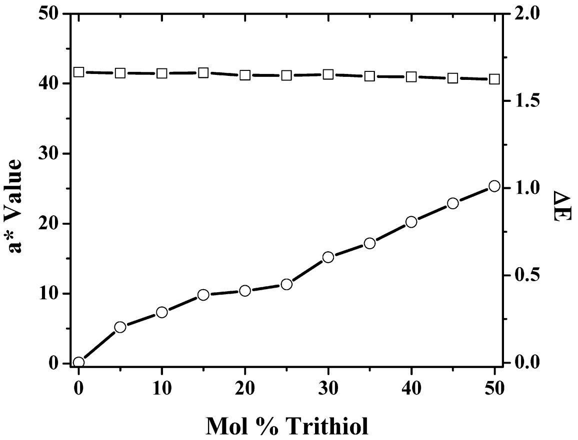

Fig. 13. Change in color parameter a^* (□) and ΔE (○) as a function of mol% trithiol content.

incident UV radiation. Trifunctional thiol significantly increases the photopolymerization rate in air and leads to higher monomer conversions. Trifunctional thiol reduces the effect of oxygen inhibition to a greater extent than traditional additives such as methyldiethanolamine, *N*-vinyl pyrrolidinone, and a novel trivinyl ester synthesized in our laboratory. AFM and colorimetry data indicate that the addition of the trifunctional thiol maintains the same level of pigment dispersion achieved with the pure acrylate. By enabling photopolymerization to take place in an air atmosphere, pigmented thiol–ene systems should prove to be an exciting area of future growth within the field of photocuring.

Acknowledgements

The authors would like to thank the National Science Foundation (Tie Grant 0120943) for funding of this research, Fusion for lamp systems, and Flint Ink Corp. for the pigment.

References

[1] Cramer NB, Davies T, O'Brien AK, Bowman CN. Macromolecules 2003;36:4631.
[2] Roper TM, Guymon CA, Hoyle CE. Polym Preprints 2003;44(1):21.
[3] Natarajan LV, Tondiglia VP, Sutherland RL, Tomlin D, Bunning TJ. Polym Mater Sci Engng 2003;89:48.
[4] Jonsson S, Cole M, Bachemin M, Nguyen C, Kuang W, Roper T, Lee T, Viswanathan K, Hoyle C. Proc Int Waterborne High-Solids, Powder Coat Symp 2003;30:295.
[5] Cramer NB, Scott JP, Bowman CN. Macromolecules 2002;35:5361.
[6] Morgan CR, Magnotta F, Ketley AD. J Polym Sci Part A: Polym Chem 1977;15:627.
[7] Gush DP, Ketley AD. Modern Paint Coat 1978;11:58.
[8] Morgan CR, Ketley AD. J Radiat Curing 1980;4:10.
[9] Kharasch MS, Nudenberg W, Mantell GJ. J Org Chem 1951;16:524.
[10] Jacobine AF. In: Fouassier JD, Rabek JF, editors. Radiation curing in polymer science and technology III. Polymerization mechanics, vol. III. London: Elsevier; 1993.
[11] Yang B. Radtech US 2000 Technical Proceedings, Baltimore, MD; 2000 p. 271.
[12] Pietschmann N. J Radiat Curing 1994;21(4):2.
[13] Hencken G. Am Inkmaker 1978;65:57.
[14] Segurola J, Allen NS, Edge M, Parrondo A, Roberts I. J Coat Technol 1999;71(894):61.
[15] Miller CW, Jonsson S, Hoyle CE, Yang D, Kuang W, Kess R, Iijima T, Nason C, Ng L. Radtech US 2000 Technical Proceedings, Baltimore, MD; 2000, p. 754.
[16] Krongauz V, Chawla CP, Woodman RK. Radtech US 2000 Technical Proceedings, Baltimore, MD; 2000, p. 260.
[17] Saithammer T. J Coat Technol 1996;68(856):41.
[18] Lee TY, Jonsson SE, Guymon CA, Hoyle CE. Polym Preprints 2003; 44(1):21.
[19] Decker C, Moussa K. J Coat Technol 1990;62(786):55.
[20] Anseth KS, Decker C, Bowman CN. Macromolecules 1995;28:4040.
[21] Cramer NB, Bowman CN. J Polym Sci Part A: Polym Chem 2001;39: 3311.
[22] Lee TY, Roper TM, Jonsson SE, Kudyakov I, Viswanathan K, Nason C, Guymon CA, Hoyle CE. Polymer 2003;44(10):2.
[23] Biggs S, Lukey AL, Spinks GM, Yau S. Prog Org Coat 2001;42:49.
[24] Tiarks F, Frechen T, Kirsch S, Leuninger J, Melan M, Pfau A, Richter F, Schuler B, Zhao CL. Macromol Symp 2002;187:739.
[25] Wicks ZW, Jone FN, Pappas SP, Organic coatings science and technology, vol. 1. New York: Wiley; 1992.